Supplemental Figures, Tables

Supplemental Table 1 – Anthropometric Data patients and unaffected controls from which iPSC were made

Cell Line	Genotype	Sex	BMI at biopsy or maximum lifetime BMI
056LB	Unaffected Control	M	19.6
1013	Unaffected Control	M	22.3
1111	Unaffected Control	F	20.6
1034	Unaffected Control	F	20.8
1043	Unaffected Control	F	19.8
1058	Unaffected Control	F	28.5
HUES42	Unaffected Control	M	n/a
031M	PWS Type 1 Large Deletion	F	15.52*
129	PWS Type 2 Large Deletion	M	49.4
139	PWS Type 1 Large Deletion	M	57.3
066MD	PWS Microdeletion	F	55.4
SWAPS1	Parthenote	Parthenote	n/a
PES2	Parthenote	Parthenote	n/a
PES5	Parthenote	Parthenote	n/a

**Patient was still in 'failure to thrive' phase at time of biopsy; maximum lifetime BMI not available.*

Supplemental Table 2 – Anthropometric Data of PWS patients, fasting controls, and PCSK1 mutation patient from which plasma glucose, proinsulin, and insulin measurements were made

SAMPLE ID	Genotype	Sub Type	Gender	BMI z-score	Age (years)	Weight (kg)
1	PWS	N/A	Male	2.69	6	28.7
2	PWS	N/A	Female	2.27	4	18.78
3	PWS	Deletion - Type 2	Female	-2.62	0.75	5.5
4	PWS	Deletion - Type 1	Female	3.80	4	16.5
5	PWS	Deletion - Type 2	Female	0.37	3	14.2
6	PWS	UPD	Male	2.71	8	43
7	PWS	Deletion - Type 1	Female	-2.12	0.75	6.17
8	PWS	UPD	Male	1.92	11	58.17
9	PWS	UPD	Male	8.32	4	32.2
10	PWS	Deletion - Type 2	Female	2.93	5.11	
11	PWS	Deletion - Type 1	Male	0.5	10.17	43.7
12	PWS	Deletion - Type 1	Male	1.87	7.35	31.8
13	PWS	Deletion - Type 2	Female	1.12	8.78	38.2
14	PWS	Deletion - Type 2	Female	2.76	7.3	48.2
15	PWS	Deletion - Type 2	Male	2.27	7.42	40.4
16	PWS	Deletion - Type 2	Female	2.63	8.04	41.1
17	Control	EMO	Male	3.08	6.01	42.4
18	Control	EMO	Female	2.11	7.7	37.4
19	Control	EMO	Female	2.47	8.76	49.5
20	Control	EMO	Male	2.88	7.49	59.4
21	Control	Sib of PWS	Female	-0.16	6.89	26
22	Control	Sib of PWS	Male	-0.94	8.42	24.5
23	Control	Sib of PWS	Male	0.94	9.23	39.6
24	Control	Sib of PWS	Female	-0.18	8.93	29.2
25	Control	EMO	Female	2.74	12.7	112.4
26	Control	EMO	Female	2.72	11.8	88.9
27	Control	EMO	Female	2.67	13	92.4
28	Control	EMO	Male	2.63	13.4	121.2
29	Control	EMO	Male	2.62	12.8	88.4
30	Control	EMO	Female	2.61	12	87.2
31	Control	EMO	Female	2.31	11.7	75.45
32	Control	EMO	Male	2.26	12.1	78.93
33	Control	EMO	Male	1.96	12	65
34	Control	EMO	Male	1.87	11.4	67.1
35	Control	Lean Control	Female	0.4	11.3	40.2
36	Control	Lean Control	Female	0.34	11.1	44.6
37	Control	Lean Control	Female	-2.07	11	27
38	Control	Lean Control	Female	-2.07	12.7	31.7
39	Control	Lean Control	Male	-2.28	11.1	30.1
40	Control	Lean Control	Female	-2.41	11.1	28.1
41	Control	Obese Control	Female	2.04	7	37.2
42	PC1 Mutation	*PCSK1* heterozygous deletion (c.71del/p.Ser24Met*73/stop codon position 72)	Male	2.92	9	110

Supplemental Table 3 – Phenotypic comparison between PWS, PWS Microdeletion, Human PC1 deficiency, PC1 deficient mouse models, Nhlh2 knockout mice, and Snord116$^{p-/m+}$ mice

Symptom/Endocrine Abnormality	**Molecular Candidate due to PC1 deficiency**	**Typical PWS Genotypes (LD, UPD) (*1*)**	**PWS MD patients (*2-6*)**	**PC1 Deficiency patients (*7*)**	**PC1 null mouse (*8, 9*)**	**PC1 N222D Mouse (*10*)**	**Nhlh2 KO mouse (*11*)**	**Snord116del mouse (*12*)**
Infantile poor weight gain/FTT	Not described in PC1 deficient patients	X (*1*)	X (*2-6*)	X - severe malabsorptive diarrhea (*7*)	X - severe runting (*8*)	Not runted	slight runting at 4-7 weeks old (*13*)	X - severe runting (*12*) *(Figure 3G)*
Developmental delay	Pro-oxytocin, proBDNF, others	X (*1*)	X (*2-6*)	Not reported	X - severe runting (*8*)	Not runted	x - slight runting at 4-7 weeks old (*13*)	X - severe runting (*12*) *(Figure 3G)*
GH Deficiency	Impaired processing ProGhrh	X (*1*)	X (*3, 5*)	X (*7*)	X (*8*)	Not runted	slight runting at 4-7 weeks old (*13*)	X *(Figure 3 G-L)*
Excessive/rapid wt gain b/w 6mo and 6yrs	Multiple candidates: POMC, proAgRP, proNPY, proCART, pro-oxytocin, proghrelin	X (*1*)	X (*2-6*)	X (*7*)	Not obese (*8*)	X (*10*)	X (*11*)	Not obese (*12*) *(Figure 3G)*
Obesity	Multiple candidates: POMC, proAgRP, proNPY, proCART, pro-oxytocin, proghrelin	X (*1*)	X (*2-6*)	X (*7*)	Not obese (*8*)	X (*10*)	X (*11*)	Not obese (*12*) *(Figure 3G)*
Hyperphagia	Multiple candidates: POMC, proAgRP, proNPY, proCART, pro-oxytocin, proghrelin	X (*1*)	X (*2-6*)	X (*7*)	Not reported	X (*10*)	X (*13*)	X - normalized to lean mass (*12*) *(Figure 3G)*
Hypogonadism	Impaired processing ProGnrh	X (*1*)	X (*2-5*)	X (*7*)	Not reported	X - slight hypogonadism, can breed but not as well and have lower testosterone (*10*)	X (*11*)	X - fertility/litter size normal, delayed vaginal opening to measure sexual maturity in females, male testosterone level not assessed (*12*)
Hyperghrelinemia	Impaired processing proghrelin	X (*1*)	X (*5*)	Not reported	Not tested	Not tested	Not tested	X - associated with impaired proghrelin processing *(Figure 3F)*

Hypoinsulinemia	Impaired processing proinsulin	X ***(14)***	Not reported	X ***(7)***	X ***(15)***	X ***(10, 16)***	Not tested	X – associated with impaired proinsulin processing ***(Figure 2B)***
Impaired processing of proinuslin to insulin	Impaired processing proinsulin	Impaired proinsulin processing, p=0.086, ***Main text Figure 2L***	Not reported	X ***(7)***	X ***(15)***	X ***(10, 16)***	Not tested	X ***(Figure 2B)***
Low circulating BDNF	Impaired processing proBDNF	X ***(17)***	Not reported	Not reported	Not tested	Not tested	Not tested	Not tested
Hypothyroidism	Impaired processing proTRH	X - literature estimates between 2%-72% PWS patients hypothyroid ***(18-20)***	X ***(5, 6)***	X ***(7)***	Not tested	Not tested	Yes decreased expression *Trh* ***(21)***	Not tested
Adrenal insufficiency	ProCRH hypothalamus, POMC pituitary	X - 60% low ACTH metyrapone response ***(22)***	Not reported	X ***(7)***	X ***(8)***	X ***(10)***	Hypothalamic POMC processing is impaired, predict pituitary POMC processing also is ***(23)***	Not tested
Cognitive impairment	May be partially explained by impaired processing proBDNF-BDNF?	X ***(1)***	X ***(2-6)***	Not reported	Not tested	Not tested	Not tested	Impaired motor learning ***(12)***
Hypopigmentation	Impaired processing POMC and/or PMCH may contribute	X ***(1)***	X ***(5)***	Not reported	Not tested	Not tested	Not tested	Not tested
Neonatal hypotonia	Not described in PC1 deficient patients	X ***(1)***	X ***(2-6)***	Not reported	Not tested	Not tested	Not tested	Not tested
PWS facial features	Not described in PC1 deficient patients	X ***(1)***	X ***(2-6)***	Not reported	n/a	n/a	n/a	n/a
Behavior problems	Pro-oxytocin, proBDNF, others	X ***(1)***	X ***(2-6)***	Not reported	Not tested	Not tested	Not tested	Not tested
Sleep disturbance	Not described in PC1 deficient patients	X ***(1)***	X ***(5)***	Not reported	Not tested	Not tested	Not tested	X - circadian genes dysregulated: *Mtor, Clock, Cry1, Per2* ***(24)***

Skin picking	Not described in PC1 deficient patients	X ***(1)***	X ***(5, 6)***	Not reported	n/a	n/a	n/a	n/a
High pain threshold	impaired processing proBDNF could contribute	X ***(1)***	Not reported	Not reported	Not tested	Not tested	Not tested	Not tested
Temperature instability	Impaired processing POMC to bEP could contribute	X ***(1)***	Not reported	Not reported	Not tested	Not tested	X ***(25)***	X
Diabetes	Impaired processing proinsulin	X ***(1)***	Not reported	X ***(7)***	X - Mild insulin resistance in *Pcsk1*$^{+/-}$ mice ***(15)***	X - Glucose intolerant ***(10)***	*Nhlh2* not expressed in islets	X - impaired proinsulin processing ***(Figure 2B)***
Neonatal Malabsorptive diarrhea	Unclear, impaired proglucagon to glp1 processing candidate	Not reported	Not reported	X ***(7)***	X – mild diarrhea ***(8)***	Not tested	Not tested	Not tested
Hypoglycemia	Impaired processing proinsulin, likely due to longer half life of proinsulin as compared to insulin	X – 12.6% with recorded hypoglycemia; repeated hypoglycemia in 83% of hypoglycemic positive patients ***(26)***	Not reported	X – can range in severity ***(7)***	IPGTT does not show hypoglycemia in *Pcsk1*$^{-/-}$ mice ***(8)***	Not hypoglycemic ***(10)***	*Ad lib* serum insulin and glucose similar between *Nhlh2* KO and WT ***(27)***	IPGTT does not show hypoglycemia in *Snord116*$^{p-/m+}$ mice ***(12)*** ***(also Figure 2A)***
Bone Mineral Density	Unclear	X ***(28)***	Not reported	Not reported	Not tested	Not tested	Not tested	Not tested
Scoliosis	Unclear	X ***(29)***	1/5 patients had mild scoliosis ***(6)***	Not reported	Not tested	Not tested	Not tested	Not tested

*Note references to existing literature for Supplemental Table 3, are formatted in ***blue, italicized, and bolded text, in parenthesis***. References to data presented in this paper are formatted in ***orange, italicized, and bolded text, in parenthesis***.

References for Supplemental Table 3:

1. M. A. Angulo, M. G. Butler, M. E. Cataletto, Prader-Willi syndrome: a review of clinical, genetic, and endocrine findings. *J Endocrinol Invest* **38**, 1249-1263 (2015).
2. T. Sahoo *et al.*, Prader-Willi phenotype caused by paternal deficiency for the HBII-85 C/D box small nucleolar RNA cluster. *Nature Genetics* **40**, 719-721 (2008).
3. A. J. de Smith *et al.*, A deletion of the HBII-85 class of small nucleolar RNAs (snoRNAs) is associated with hyperphagia, obesity and hypogonadism. *Human molecular genetics* **18**, 3257-3265 (2009).
4. A. L. Duker *et al.*, Paternally inherited microdeletion at 15q11.2 confirms a significant role for the SNORD116 C/D box snoRNA cluster in Prader-Willi syndrome. *European journal of human genetics : EJHG* **18**, 1196-1201 (2010).
5. E. Bieth *et al.*, Highly restricted deletion of the SNORD116 region is implicated in Prader-Willi Syndrome. *Eur J Hum Genet* **23**, 252-255 (2015).

6. M. G. Butler, S. L. Christian, T. Kubota, D. H. Ledbetter, A 5-Year-Old White Girl with Prader-Willi Syndrome and a Submicroscopic Deletion of Chromosome 15q11q13. *American Journal of Medical Genetics* **65**, 137-141 (1996).
7. P. Stijnen, B. Ramos-Molina, S. O'Rahily, J. W. M. Creemers, PCSK1 mutations and human endocrinopathies: from obesity to gastrointestinal disorders. *Endocrine Reviews* **17**, (2016).
8. X. Zhu *et al.*, Disruption of PC1/3 expression in mice causes dwarfism and multiple neuroendocrine peptide processing defects. *Proceedings of the National Academy of Sciences of the United States of America* **99**, 10293-10298 (2002).
9. X. Zhu, Y. Cao, K. Voogd, D. F. Steiner, On the processing of proghrelin to ghrelin. *The Journal of biological chemistry* **281**, 38867-38870 (2006).
10. D. J. Lloyd, S. Bohan, N. Gekakis, Obesity, hyperphagia and increased metabolic efficiency in Pc1 mutant mice. *Human molecular genetics* **15**, 1884-1893 (2006).
11. F. D. P. Deborah J. Good, Kathleen A. Mahon, Albert F. Parlow, Heiner Westphal, Ilan R. Kirsch, Hypogonadism and obesity in mice with a targeted deletion of the Nhlh2 gene. *Nature Genetics* **15**, 397-401 (1997).
12. F. Ding *et al.*, SnoRNA Snord116 (Pwcr1/MBII-85) deletion causes growth deficiency and hyperphagia in mice. *PloS one* **3**, e1709-e1709 (2008).
13. C. A. Coyle. *et al.*, Reduced voluntary activity precedes adult-onset obesity in Nhlh2 knockout mice. *Physiology & Behavior* **77**, 387-402 (2002).
14. A. M. Haqq, M. J. Muehlbauer, C. B. Newgard, S. Grambow, M. Freemark, The metabolic phenotype of Prader-Willi syndrome (PWS) in childhood: heightened insulin sensitivity relative to body mass index. *The Journal of clinical endocrinology and metabolism* **96**, E225-232 (2011).
15. X. Zhu. *et al.*, Severe block in processing of proinsulin to insulin accompanied by elevation of des-64,65 proinsulin intermediates in islets of mice lacking prohormone convertase 1/3. *Proceedings of the National Academy of Sciences* **99**, 10299–10304 (2002).
16. P. Stijnen *et al.*, Endoplasmic reticulum-associated degradation of the mouse PC1/3-N222D hypomorph and human PCSK1 mutations contributes to obesity. *International Journal of Obesity* **40**, 973-981 (2016).
17. J. C. Han, M. J. Muehlbauer, H. N. Cui, C. B. Newgard, A. M. Haqq, Lower Brain-Derived Neurotrophic Factor in Patients with Prader-Willi Syndrome Compared to Obese and Lean Control Subjects. *J Clin Endocrinol Metab* **95**, 3532-3536 (2010).
18. E. Vaiani *et al.*, Thyroid axis dysfunction in patients with Prader-Willi syndrome during the first 2 years of life. *Clinical Endocrinology* **73**, 546-550 (2010).
19. J. L. Miller *et al.*, Pituitary abnormalities in Prader-Willi syndrome and early onset morbid obesity. *American Journal of Medical Genetics* **146A**, 570-577 (2008).
20. M. G. Butler, M. Theodoro, J. D. Skouse, Thyroid Function Studies in Prader-Willi Syndrome. *American Journal of Medical Genetics Part A* **143A**, 488-492 (2007).
21. K. R. Vella, A. S. Burnside, K. M. Brennan, D. J. Good, Expression of the hypothalamic transcription factor Nhlh2 is dependent on energy availability. *Journal of Neuroendocrinology* **19**, 499-510 (2007).
22. R. F. de Lind van Wijngaarden *et al.*, High prevalence of central adrenal insufficiency in patients with Prader-Willi syndrome. *J Clin Endocrinol Metab* **93**, 1649-1654 (2008).
23. E. Jing, E. A. Nillni, V. C. Sanchez, R. C. Stuart, D. J. Good, Deletion of the Nhlh2 transcription factor decreases the levels of the anorexigenic peptides alpha melanocyte-stimulating hormone and thyrotropin-releasing hormone and implicates prohormone convertases I and II in obesity. *Endocrinology* **145**, 1503-1513 (2004).
24. W. T. Powell *et al.*, A Prader–Willi locus lncRNA cloud modulates diurnal genes and energy expenditure. *Human Molecular Genetics* **22**, 4318-4328 (2013).
25. U. D. Wankhade, K. R. Vella, D. L. Fox, D. J. Good, Deletion of Nhlh2 Results in a Defective Torpor Response and Reduced Beta Adrenergic Receptor Expression in Adipose Tissue. *PLoS One* **5**, e12323 (2010).
26. R. A. Harrington, D. A. Weinstein, J. L. Miller, Hypoglycemia in Prader-Willi syndrome. *Am J Med Genet A* **164A**, 1127-1129 (2014).
27. D. L. Fox, Dissertation, University of Massachusetts Amherst, Ann Arbor, MI (2007).
28. M. G. Butler *et al.*, Decreased bone mineral density in Prader-Willi syndrome: comparison with obese subjects. *American Journal of Medical Genetics Part A* **103**, 216-222 (2001).
29. T. Odent *et al.*, Scoliosis in Patients With Prader-Willi Syndrome. *Pediatrics* **122**, 1-7 (2008).

Supplemental Table 4 – Primers

Human			
Gene Name	Forward	Reverse	Source/Reference
TBP	TGCACAGGAGCCAAGAGTGAA	CACATCACAGCTCCCCACCA	Primer sequences provided by Dr. Andrew Sproul.
MAGEL2	CCTGGGCTCCGCTAAATCATT	TCATGCGGTCTTTTGAAGGGG	Designed using NCBI primer blast.
SNRPN	CTGCAAACATAGGAGATGATAGTTCC	CAAAGACGATAAAATGTTCCTTCTTG	Designed using NCBI primer blast.
SNORD109	ATAATTGTCTGAGGATGCT	GATTGACATCTGGAATGAGTC	Designed using NCBI primer blast.
SNORD116	CGATGATGAGTCCCCCATAAAAAC	CAGTTCCGATGAGAACGACG	Primer sequences provided by Dr. Daniel Driscoll's laboratory.
IPW	TGCCTAGACCACCCACTAAAGG	AGTCTCCATGCGGAAGGAAGA	Stelzer, Y. *et al.* Nature Genetics. 2014.
NHLH2	GTCCGGACTCAGCATCATTT	ATATTTTCCGGAATCTCCCCT	Wang, L., *et al.* JCI. 2016.
PCSK1	ACCAGGTGCTGCATATCTCG	CACAATGACTGCACGGAGAC	Wang, L., *et al.* JCI. 2016.
PCSK2	TTTCGGTCAAATCCTTCCTG	TGCAAAGGCCAAGAGAAGAC	Wang, L., *et al.* JCI. 2016.
POMC	GACACTGGCTGCTCTCCAG	AGCAGCCTCCCGAGACA	Wang, L., *et al.* JCI. 2016.
FURIN	CCTGGTTGCTATGGGTGGTAG	AAGTGGTAATAGTCCCCGAAGA	Sun, G., *et al.* JBC. 2015.
CPE	CTTGGCCCAGTACCTATGCAA	ACCAGTCCTTGAGTTCACCAG	Designed using NCBI primer blast.
Mouse			
Bact	CGGGCTGTATTCCCCTCCA	GGGCCTCGTCACCCACATAG	Designed using NCBI primer blast.
Snord116	TGGATCTATGATGATTCCCAG	TGGACCTCAGTTCCGATGAG	Ding, F., *et al.* PloS One. 2008.
Nhlh2	GTGTCGGACCTAGAGCCAGT	GAGGCAGCGTGGGTAGTAGT	Primer sequences provided by Dr. Deborah Good.
Pcsk1	TCACAAGTGTGGGGTTGGAG	GGTCCCCTCCCACCATTTTAT	Designed using NCBI primer blast.
Pcsk2	CTGTTCAACACTGGGAAAGC	TCCGCCGCCCATTCATTAAC	Designed using NCBI primer blast.
Ghrl	CCATCTGCAGTTTGCTGCTA	GCTTGTCCTCTGTCCTCTGG	Ejarque, M. *et al*. PLoS One. 2016.
Igf1	GCTGGTGGATGCTCTTCAGTT	GGTGCCCTCCGAATGCT	Ding, F., *et al.* PloS One. 2008.
Lep	TGACACCAAAACCCTCATCA	AGCCCAGGAATGAAGTCCA	Guo, K., *et al*. Nutr. Metab. 2010.
LepRb	AACCCCAAGAATTGTTCCTGG	GGAGACCATAGCTGCTGGGACC	Stratigopoulos, G. Cell Metab. 2014.
Ins2	GCTTCTTCTACACACCCATGTC	AGCACTGATCTACAATGCCCAC	Abdellatif, A., *et al.* Exp. Anim. 2015.

References for primers (*12*, *30-36*).

Supplemental Figure 1

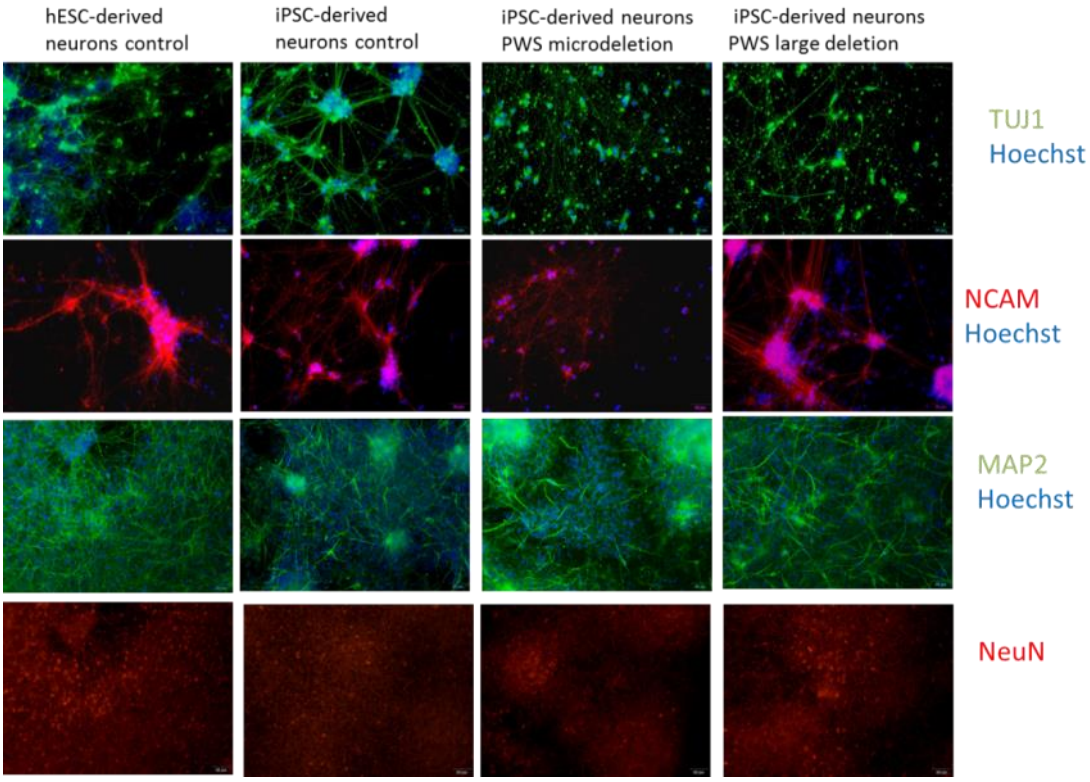

Supplemental Figure 1: PWS and unaffected control iPSC-derived neurons express pan-neuronal markers. PWS and unaffected control iPSC were differentiated to iPSC-derived neurons using a modified dual SMAD inhibition protocol; staining was performed at day 34 of differentiation. β-III-tubulin (TUJ1) and neural cell adhesion molecule (NCAM) mark neuronal cell bodies and processes. MAP2 marks post-mitotic neurons, NeuN marks neuronal nuclei. Images are all 20X.

Supplemental Figure 2

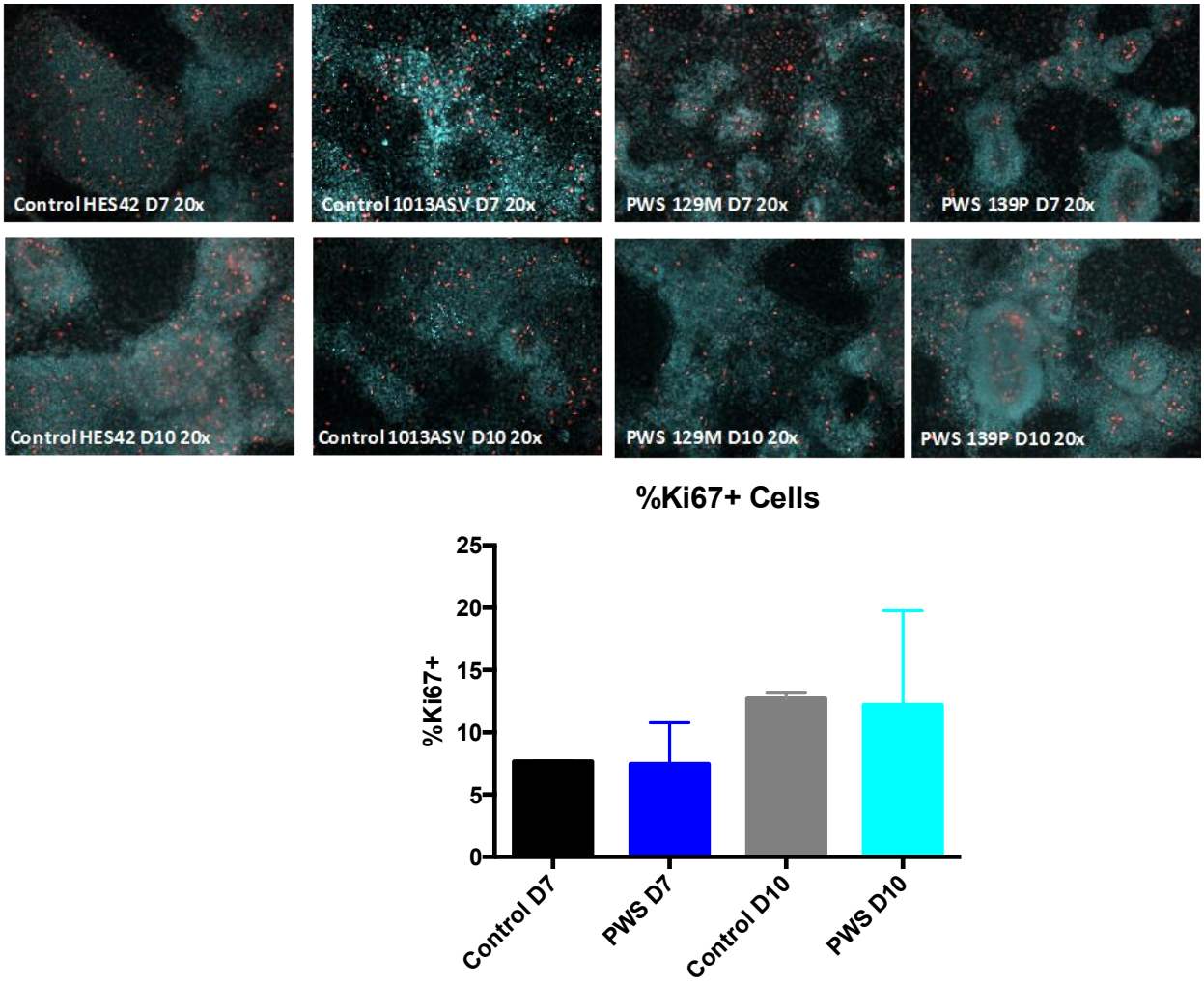

Supplemental Figure 2: There is no difference in the percentage of Ki67 positive cells during neuronal differentiation between PWS and unaffected control genotypes. Unaffected control hESC (HES42), unaffected control iPSC (1013ASV) and PWS iPSC (129M and 139P) were subjected to neuronal differentiation. Ki67 staining was performed at days 7 (D7) and 10 (D10) of differentiation. There is no difference in the percentage of Ki67 positive cells in the culture. Ki67 is a marker of proliferating cells and is shown in red while DAPI marks DNA and is shown in cyan in all micrographs above. Images are all 20X.

Supplemental Figure 3

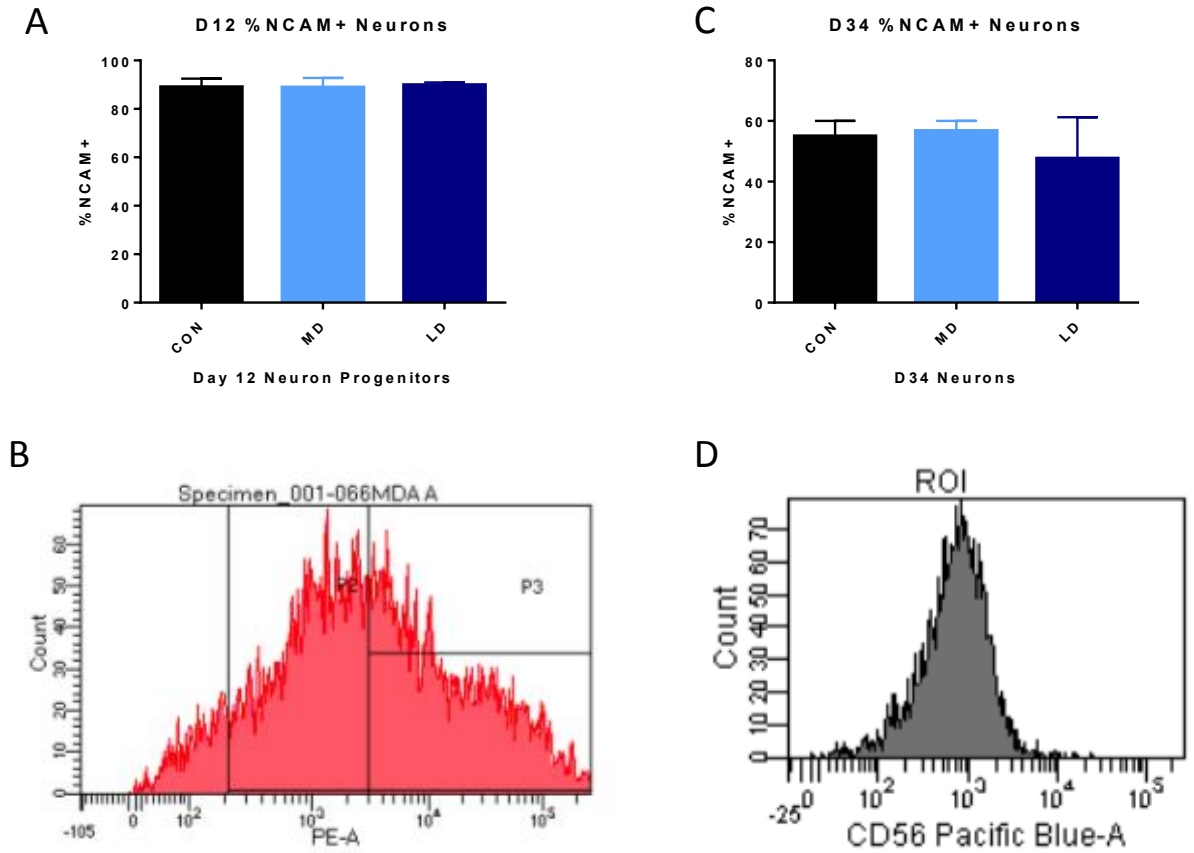

Supplemental Figure 3: There is no difference in the percentage of NCAM+ cells at day 12 and day 34 of neuronal differentiation between unaffected control and PWS genotypes. Unaffected control, PWS microdeletion, and PWS large deletion iPSC were differentiated to neurons and analyzed for the percentage of NCAM (also known as CD56) positive cells at days 12 and 34 of differentiation by fluorescence activated cell sorting (FACS). A) There is no difference in the percentage of NCAM+ cells at day 12 of differentiation (n=5 unaffected control PSC lines, n=1 PWS microdeletion line (3 clones used), n=2 PWS large deletion lines). B) A representative FACS plot of NCAM fluorescence intensity at day 12 of differentiation. C) There is no difference in the percentage of NCAM+ cells at day 34 of differentiation (n=7 unaffected control PSC, n=1 PWS microdeletion (2 clones used), n=3 PWS large deletion). D) A representative FACS plot of NCAM fluorescence intensity at day 34 of sorting.

Supplemental Figure 4:

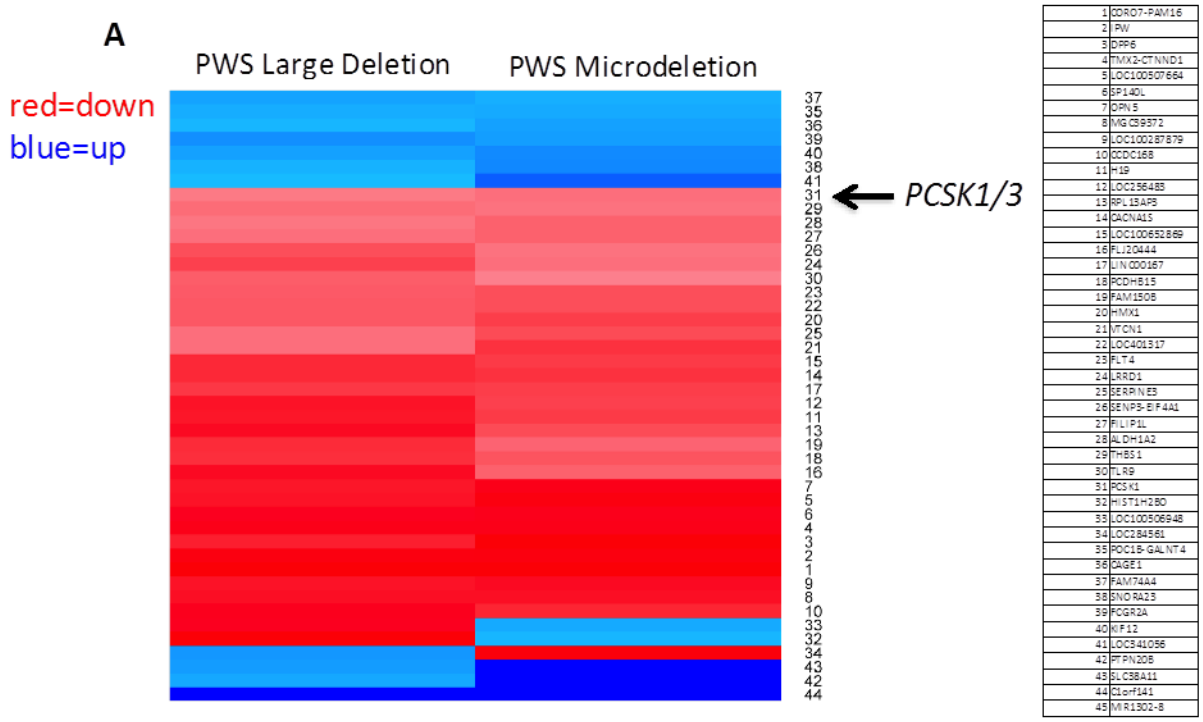

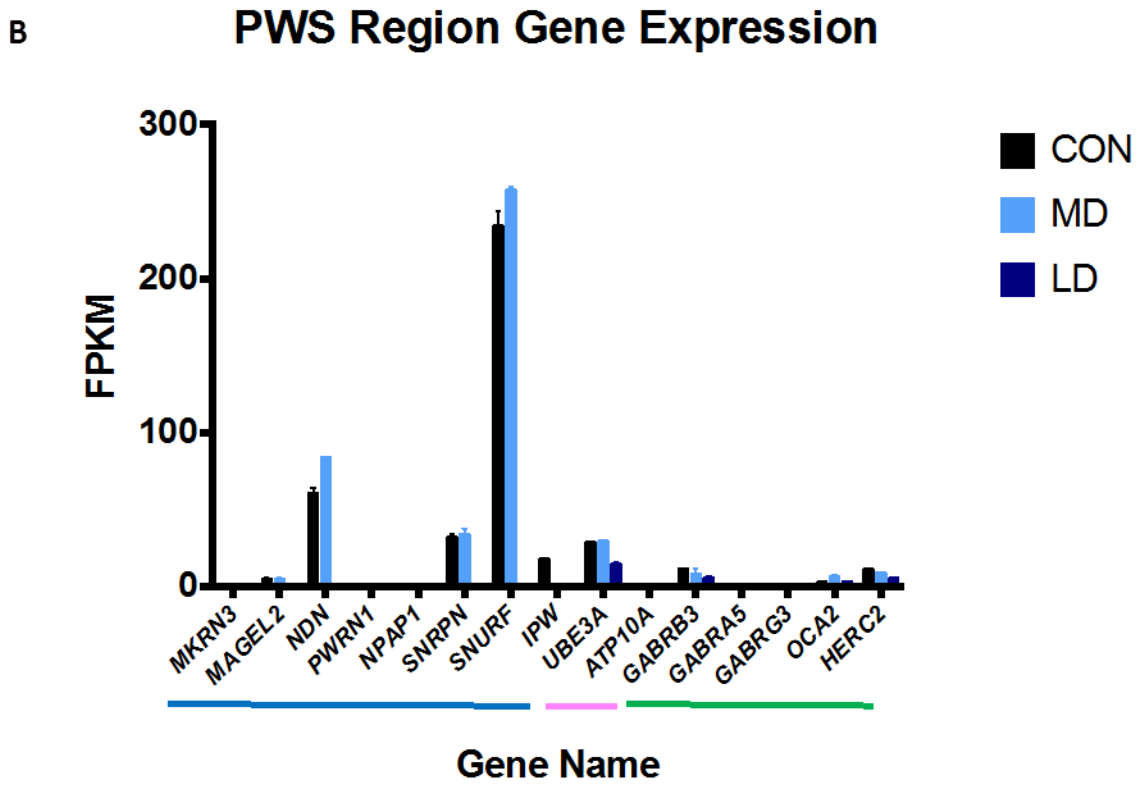

Supplemental Figure 4: RNA sequencing identifies downregulation of *PCSK1* in PWS iPSC-derived neurons. A) Differentially expressed genes common between Microdeletion PWS and Large Deletion PWS genotypes as compared to unaffected control genotypes (Student t test, 2 tailed, type 3, without Bonferroni correction; no genes were significant with Bonferroni correction). Forty-five genes were differentially expressed in both PWS genotypes. Of the 45 differentially expressed genes, 42 were differentially expressed in the same direction, including *IPW* and LOC1005069 from the PWS locus; snoRNA genes are not picked up by the RNA sequencing package used, 30 million, 100 bp reads. *PCSK1* (also known as *PCSK1/3*) is downregulated by 51% and 61% in microdeletion and large deletion, respectively ($P<0.05$). The heat map of **Supplemental Figure 4A** is also shown in the **Main Text Figure 1G**. We show this heat map

twice because in **Supplemental Figure 4A** we provide the full list of gene names, whereas in **Main Text Figure 1G**, we highlight the downregulation of *PCSK1*. B) Gene expression in the PWS region in unaffected control (CON), PWS microdeletion (MD), and PWS large deletion (LD) NCAM+ iPSC-derived neurons as measured by RNA sequencing. PWS region genes remain appropriately silenced in PWS iPSC-derived neurons. PWS region genes are expressed in unaffected control iPSC-derived neurons. The green line denotes non-imprinted genes, the pink line denotes maternally-expressed genes, and the blue line denotes paternally-expressed genes (n=7 unaffected control PSC, n=1 PWS microdeletion (2 clones used), n=2 PWS large deletion).

Category	Term	Count	%	PValue	Genes
SP_PIR_KEYWORDS	**glycoprotein**	12	34.28571	0.01	**OPN5, PCSK1, VTCN1, SERPINE3, FLT4, PCDHB15, SLC38A11, FCGR2A, DPP6, THBS1, CACNA1S, TLR9**
SP_PIR_KEYWORDS	**signal**	9	25.71429	0.03	**PCSK1, VTCN1, SERPINE3, FLT4, PCDHB15, FCGR2A, FAM150B, THBS1, TLR9**
SP_PIR_KEYWORDS	receptor	6	17.14286	0.04	OPN5, FLT4, FCGR2A, PTPN20B, CACNA1S, TLR9
SP_PIR_KEYWORDS	**disulfide bond**	8	22.85714	0.05	**OPN5, PCSK1, VTCN1, FLT4, FCGR2A, DPP6, THBS1, CACNA1S**

Category	Term	Count	%	PValue	Genes
UP_SEQ_FEATURE	**glycosylation siteN-linked (GlcNAc...)**	12	34.28571	0.00	**OPN5, PCSK1, VTCN1, SERPINE3, FLT4, PCDHB15, SLC38A11, FCGR2A, DPP6, THBS1, CACNA1S, TLR9**
UP_SEQ_FEATURE	topological domainExtracellular	9	25.71429	0.01	OPN5, VTCN1, FLT4, PCDHB15, SLC38A11, FCGR2A, DPP6, CACNA1S, TLR9
UP_SEQ_FEATURE	**signal peptide**	9	25.71429	0.03	**PCSK1, VTCN1, SERPINE3, FLT4, PCDHB15, FCGR2A, FAM150B, THBS1, TLR9**
UP_SEQ_FEATURE	topological domainCytoplasmic	9	25.71429	0.04	OPN5, VTCN1, FLT4, PCDHB15, SLC38A11, FCGR2A, DPP6, CACNA1S, TLR9

Category	Term	Count	%	PValue	Genes
GOTERM_BP_FAT	**GO:0048545~response to steroid hormone stimulus**	3	8.571429	0.02	**ALDH1A2, PCSK1, THBS1**
GOTERM_BP_FAT	**GO:0021983~pituitary gland development**	2	5.714286	0.03	**ALDH1A2, PCSK1**
GOTERM_BP_FAT	**GO:0031016~pancreas development**	2	5.714286	0.04	**ALDH1A2, PCSK1**
GOTERM_BP_FAT	**GO:0021536~diencephalon development**	2	5.714286	0.04	**ALDH1A2, PCSK1**

Supplemental Table 6: Results of DAVID pathway analysis for iPSC-derived neurons. Unaffected control is compared to PWS microdeletion and PWS large deletion. Most of the pathways that the DAVID software identified as being dysregulated include *PCSK1*.

Supplemental Figure 5

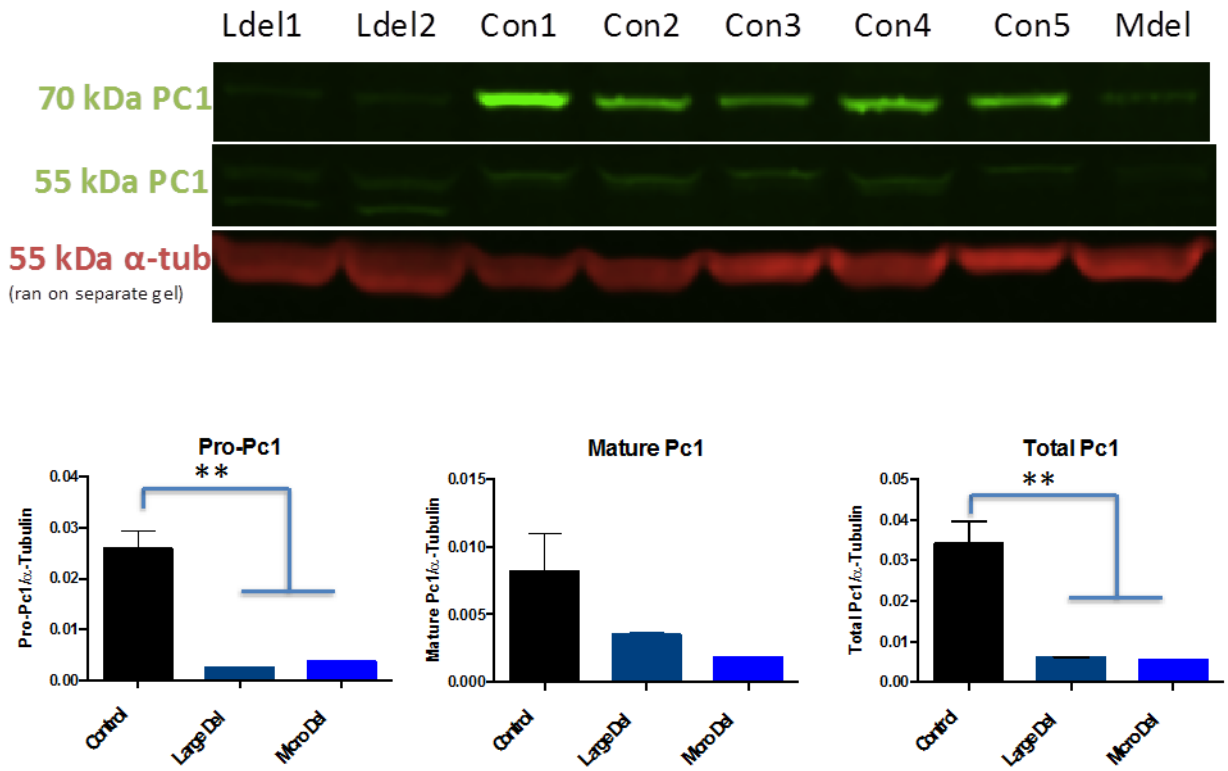

Supplemental Figure 5: PC1 protein is downregulated in PWS iPSC-derived neurons compared to unaffected control iPSC-derived neurons. Quantification is shown in Main Text Figure 1. Day 34 neurons were probed for PC1 protein levels by western blotting. (n=5 controls (3 lines), n=2 PWS large deletion, n=1 PWS microdeletion; error bars SEM). Ldel = PWS large deletion, Mdel = PWS microdeletion, Con = Control.

Supplemental Figure 6

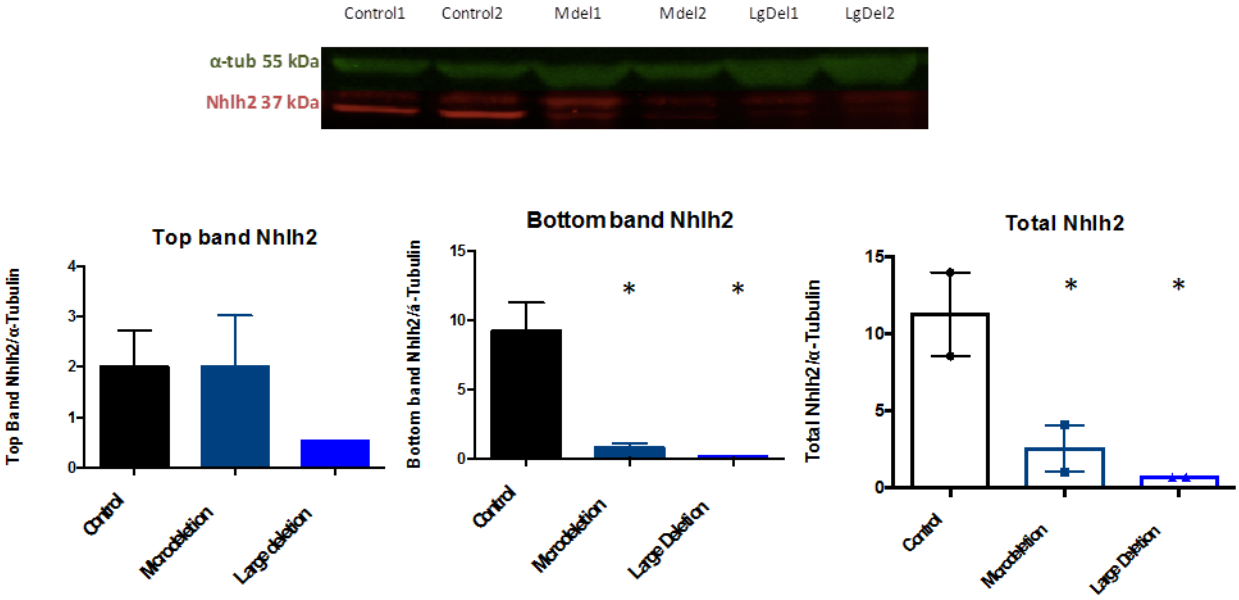

Supplemental Figure 6: Nhlh2 protein is down-regulated in PWS iPSC-derived neurons compared to unaffected control iPSC-derived neurons. Quantification is shown in Main Text Figure 1. Day 34 neurons were probed for Nhlh2 protein levels by western blotting. (n=2 unaffected control lines, 2 PWS microdeletion clones, 2 PWS large deletion lines; 1-way ANOVA, Tukey/Fishers Post hoc test, *=P<0.05, Error bars are SEM). Lgdel = PWS large deletion, Mdel = PWS microdeletion.

Supplemental Figure 7

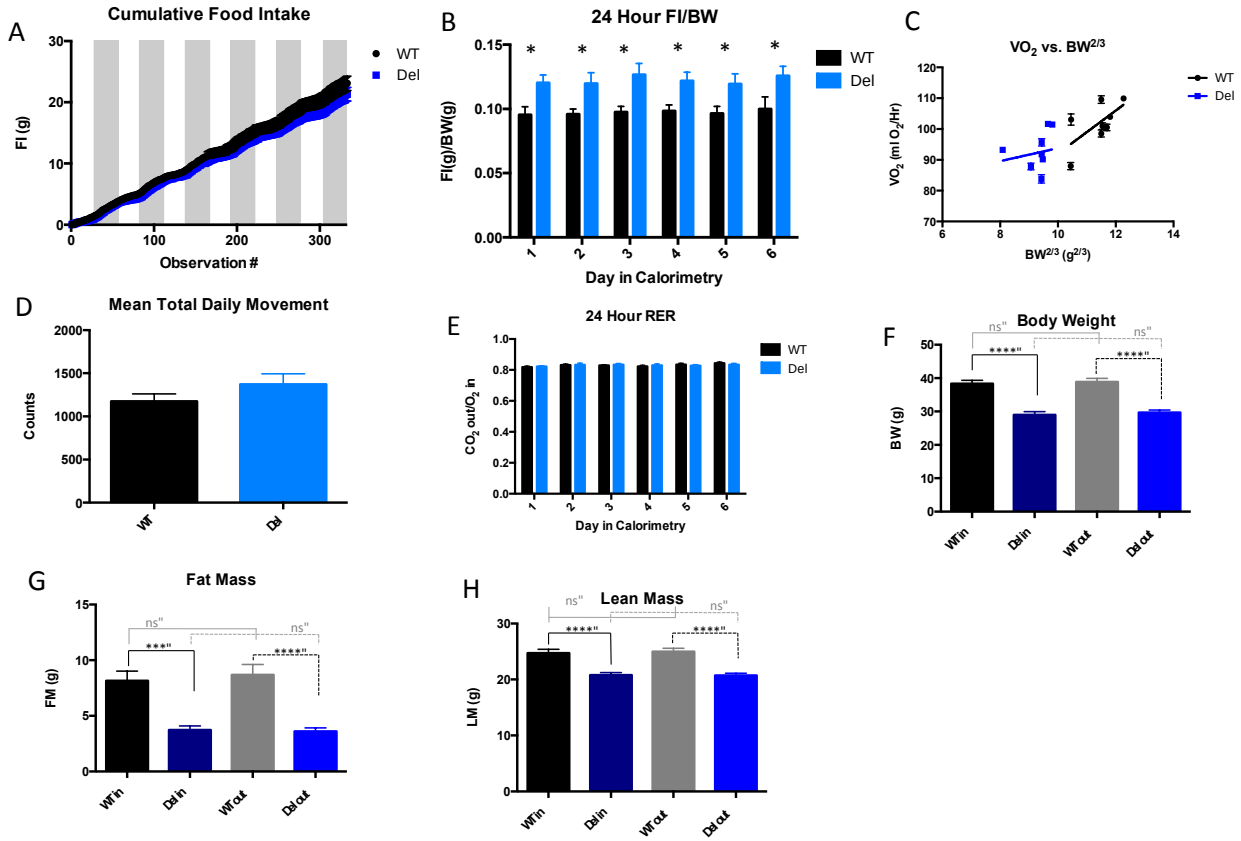

Supplemental Figure 7: Long-term cumulative food intake of Snord116$^{p-/m+}$ mice does not differ from WT despite decreased body size and weight. A) Cumulative food intake is not different between 20 week old male Snord116$^{p-/m+}$ mice and WT littermates, despite 24% lower body weight and 16% lower lean mass of Snord116$^{p-/m+}$ mice. Error bars are SEM Unpaired t-test, n=10 wt, n=9 deletion, 6 mo males. B) When 24 hour food intake is expressed in proportion to body weight, Snord116$^{p-/m+}$ mice consume ~ 25% more than WT. C) When energy expenditure is plotted against BW$^{2/3}$, a single linear regression equation can be used to describe both Snord116$^{p-/m+}$ and WT data sets, suggesting that the increased energy expenditure of Snord116$^{p-/m+}$ mice may be accounted for by increased heat loss due to higher surface area to body mass ratio of Snord116$^{p-/m+}$ animals. The same result is also found when plotting VO_2 against FFM. (Data were plotted as a non-linear regression using least squares (ordinary fit), extra sum of squares F-test was used to determine best-fit values of unshared parameters differed between the 2 data sets (WT and DEL), the null hypothesis was not rejected (p=0.09) n=8 wt, n=8 deletion, 6 mo males.) D) Mean daily movement is not different between Snord116$^{p-/m+}$ and WT mice. E) There is no change in the 24 hour respiratory exchange (RER) ratio between Snord116$^{p-/m+}$ and WT mice; there is also no difference between light cycle and dark cycle RER amongst genotypes (data not shown). F) Snord116$^{p-/m+}$ mice have decreased body weight as compared to WT littermates; there is no change in body weight before and after time in the metabolic cage within genotype. G) Fat mass is decreased in Snord116$^{p-/m+}$ mice; there is no change in fat mass before and after time in the metabolic cage within genotype. H) Snord116$^{p-/m+}$ mice have decreased lean mass as compared to WT littermates; there is no change in lean mass before and after time in the metabolic cage within genotype.

Supplemental Figure 8

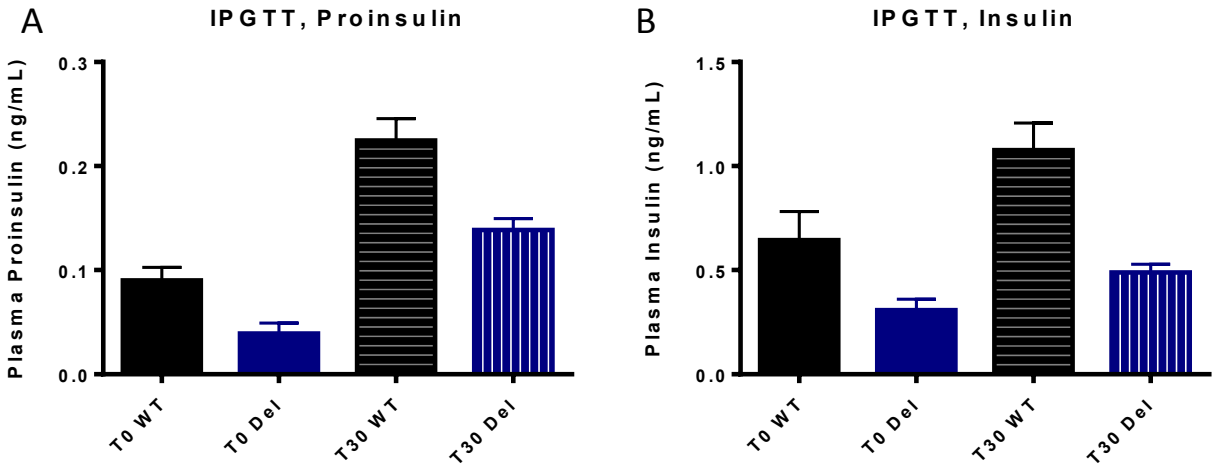

Supplemental Figure 8: A disproportionate reduction in insulin levels 30 minutes following glucose injection accounts for the increase in the proinsulin to insulin ratio in Snord116$^{p-/m+}$ (Del) mice. Blood glucose levels and proinsulin to insulin ratio is shown in main text Figure 3A-B (n=9 WT, n=7 Snord116$^{p-/m+}$ mice).

Supplemental Figure 9

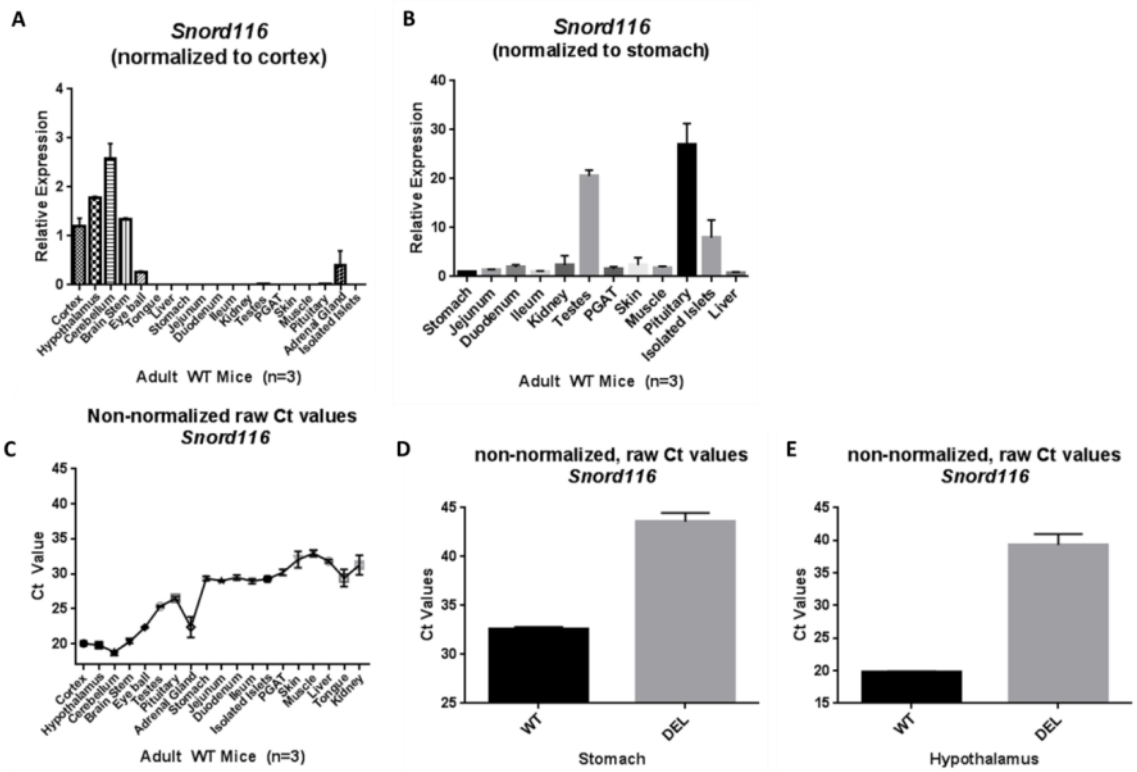

Supplemental Figure 9: Across tissue expression analysis of *Snord116* in Wild Type mice. A-C) The highest levels of *Snord116* expression are in the brain, however, it is expressed in the periphery with many tissues, including eyes, testes, pituitary, adrenal gland, stomach, jejunum, duodenum, ileum, and isolated islets having Ct values breaking between 20 and 29. D) There is a large difference in Ct values for *Snord116* between WT and *Snord116*$^{p-/m+}$ in the stomach further supporting that *Snord116* is expressed in the stomach of WT mice. E) There is a large difference in Ct values between WT and *Snord116*$^{p-/m+}$ in the hypothalamus for *Snord116.* Note that when no expression is detected Ct values are assumed to equal 45 for purposes of analysis.

Supplemental Figure 10

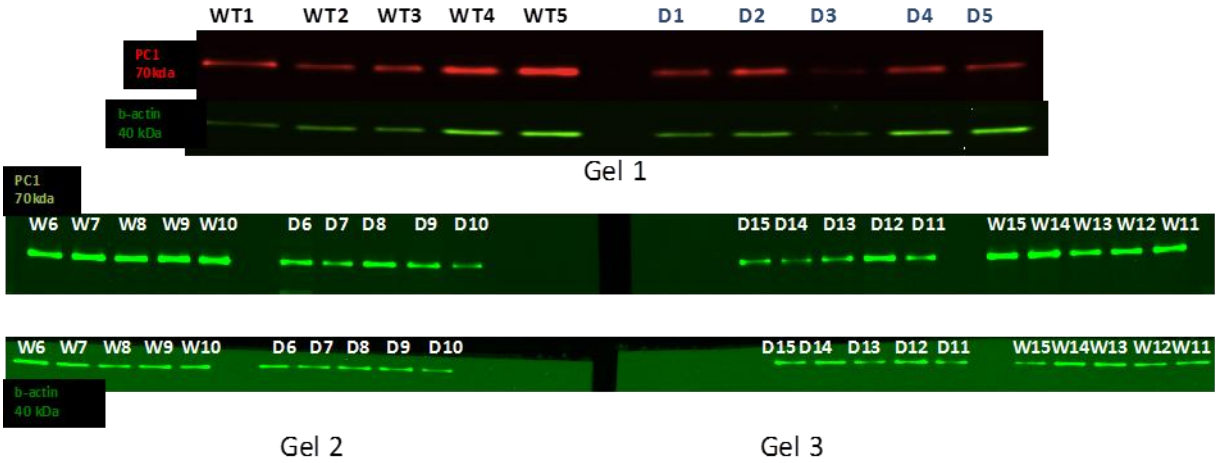

Supplemental Figure 10: PC1 protein levels are reduced in Snord116$^{p-/m+}$ islets. Quantification is shown in Main Text Figure 2.

Supplemental Figure 11

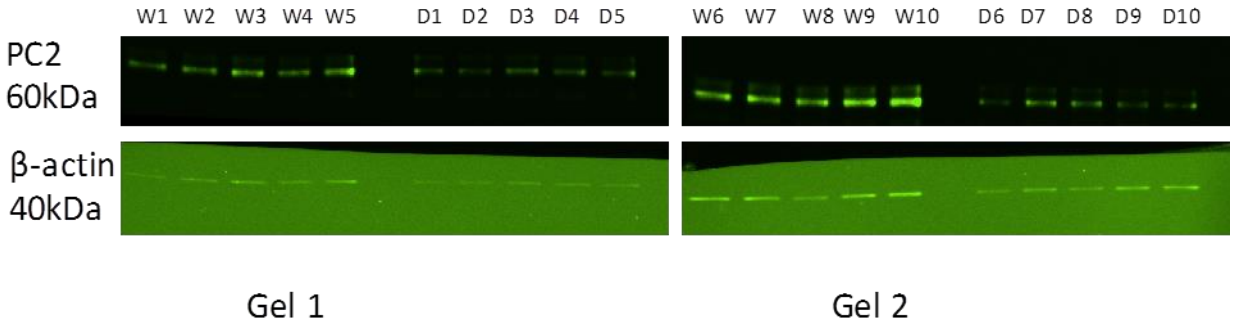

Supplemental Figure 11: PC2 protein levels are reduced in Snord116$^{p-/m+}$ islets. Quantification is shown in Main Text Figure 2.

Supplemental Figure 12

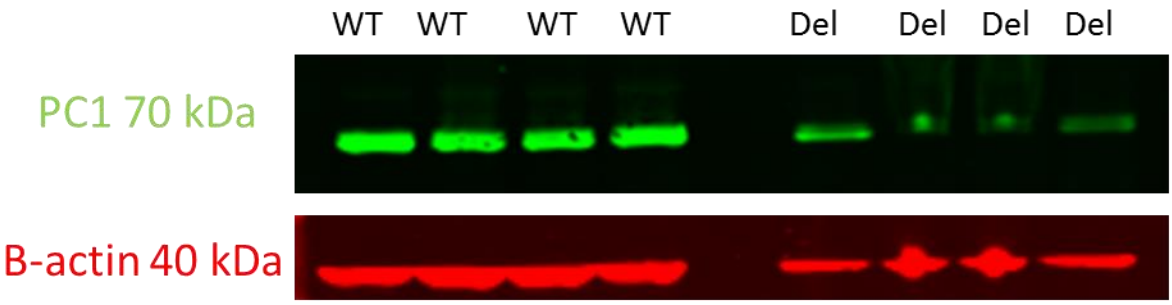

Supplemental Figure 12: PC1 protein levels trend towards a decrease in Snord116$^{p-/m+}$ stomachs. Quantification is shown in Main Text Figure 3.

Supplemental Figure 13

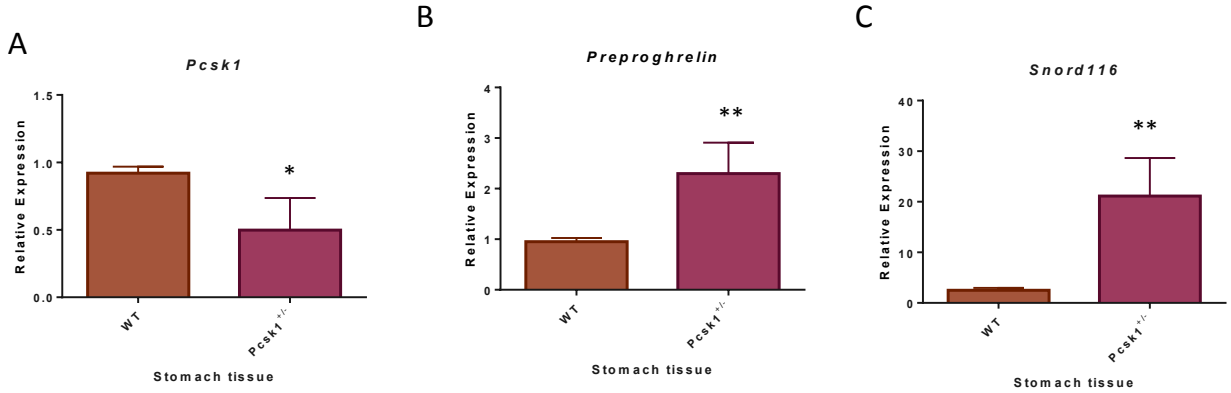

Supplemental Figure 13: *Snord116* expression is upregulated in stomachs of PC1$^{+/-}$ mice. A) *Pcsk1* expression in the stomach is downregulated 50% in mice that are heterozygous for *Pcsk1*. B) *Ghrl*, which encodes the full length, unprocessed *Preproghrelin*, is upregulated in stomachs of *Pcsk1*$^{+/-}$ mice compared to WT, suggesting that just a 50% reduction in *Pcsk1* levels are sufficient for increased *Ghrl* expression. C) *Snord116* expression is increased greater than 10-fold in the stomachs of *Pcsk1*$^{+/-}$ mice compared to WT, suggesting a negative feedback mechanism.

Supplemental Figure 14

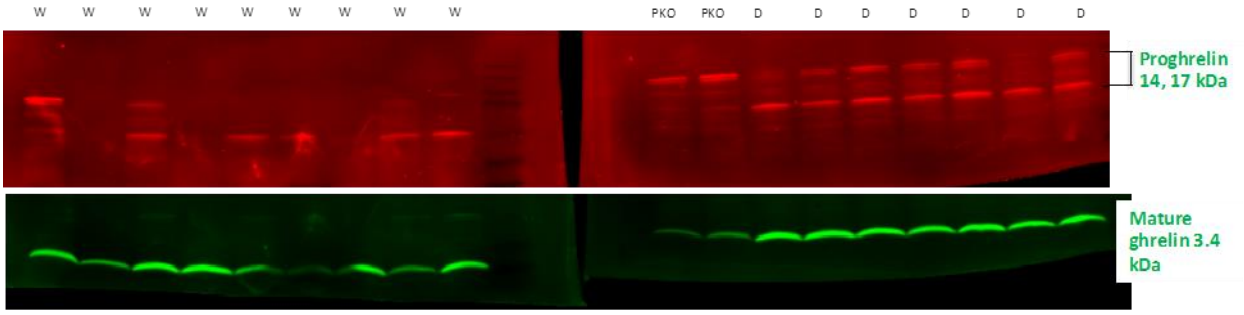

Supplemental Figure 14: Processing of proghrelin to mature ghrelin is impaired in Snord116$^{p-/m+}$ mouse stomach lysates. Quantification is shown in Main Text Figure 3. Red bands at 12 to 17 kDa are preproghrelin. Green bands at 3.4 kDa are mature ghrelin. Imaging was done using the Licor Odyssey two color imaging system; blots were probed for mature ghrelin and preproghrelin separately using two different antibodies, anti-ghrelin and anti-preproghrelin, respectively. Bands at 12-17 kDa and 3.4 kDa below are from the same blots and same gel lanes (W = wild type, PKO = PC1 null, D = Snord116 deletion; n=9 W; n=7 D; n=2 PKO; adult mice fasted overnight). Note, blots are cropped here to show regions from which quantification was done. Full blots are shown in the following figure, Supplemental Figure 21; top is H-0310-34 Phoenix Peptide anti preproghrelin antibody, bottom is Santa Cruz C-18 anti ghrelin antibody. Note also that due to the stomach lysate preparation methodology to probe for ghrelin (see methods) in which the hydrophobic supernatant fraction is taken following acetone precipitiation, typical loading controls such as α-tubulin or β-actin are not present in this fraction. Hydrophobic proteins that might be used as a loading control such as pan-cadherin or Sodium Potassium ATPase were tried but could not be identified by western blotting in this lysate fraction. Thus, the most relevant comparison here is the ratio of proghrelin to mature ghrelin; absolute quantities of proghrelin or mature ghrelin in *Snord116*$^{p-/m+}$ compared to WT are difficult to interpret without a proper loading control.

Supplemental Figure 15 (2 pages)

A

H-031-34 Pheonix peptide antibody
Against proghrelin domain that specifically gets cleaved off by PC1; epitope also crosses cleavage area.

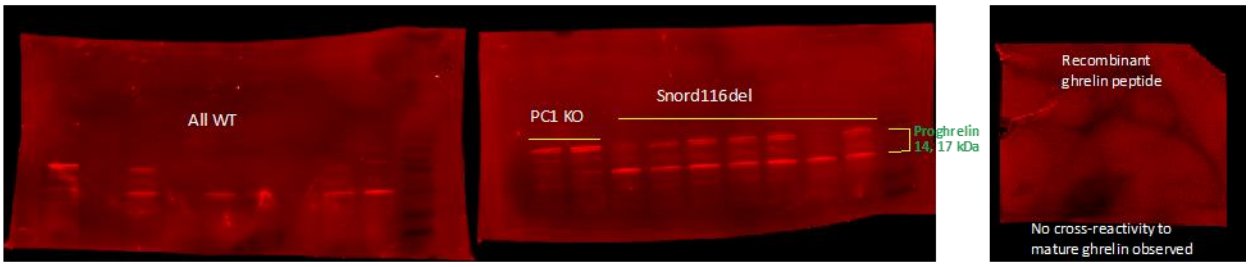

H-031-034 preproghrelin human antibody (HUMAN) (86-117) epitope:
LSGVQYQQHSQALGKFLQNILWKKAKEAPANK

Mouse sequence: yellow highlighted where the ab matches
MLSSGTICSLLLLSMLWMDMAMAGSSFLSPEHQKAQFNAPFDVGIKLSGAQYQQHGRALGKFLQDILWEEVKEAPADK
Red = signal sequence res 1-23; Black = ghrelin res 24-51; Blue = c-terminal peptide res 52-78

B

SC10368 Santa Cruz anti-ghrelin c-18 antibody
Targeted against internal epitope between residues 25-75 of human ghrelin sequence with predicted reactivity also to mouse.

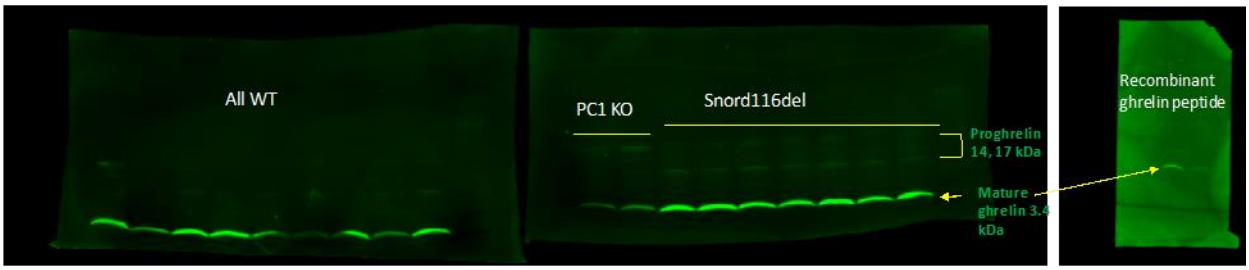

Exact epitope reactivity considered proprietary
Between 25 and 75 of the human sequence
Accession #: Q9UBU3

```
    10         20         30         40         50
MPSPGTVCSL LLLGMLWLDL AMAGSSFLSP EHQRVQQRKE SKKPPAKLQP
        60         70         80         90        100
RALAGWLRPE DGGQAEGAED ELEVRFNAPF DVGIKLSGVQ YQQHSQALGK
       110
FLQDILWEEA KEAPADK
```

C

H-031-31 Phoenix peptide antibody
Against full mature mouse ghrelin peptide

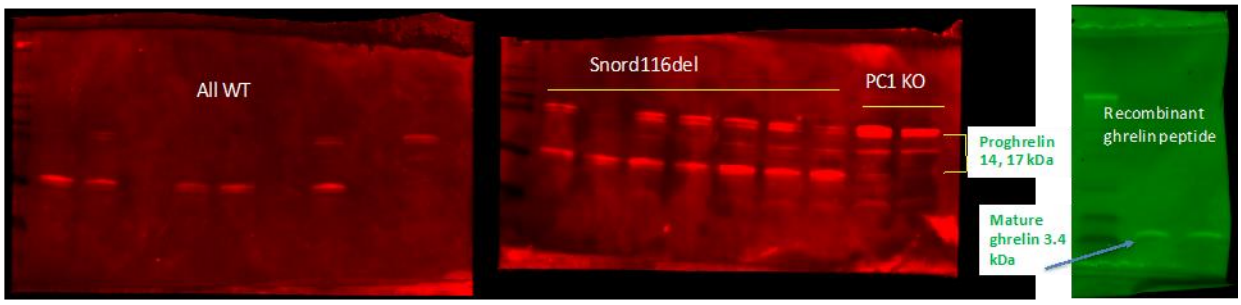

H-031-031 Ghrelin (Rat, mouse) antibody
GSSFLSPEHGKAQQRKESKKPPAKLQPR
Mouse sequence: BLUE highlighted where the ab matches
MLSSGTICSLLLLSMLWMDMAMAGSSFLSPEHQKAQQRKESKKPPAKLQPRALEGWLHPEDRG....EEVKEAPADK
Red = signal sequence res 1-23; Black = ghrelin res 24-51; Blue = c-terminal peptide res 52-78

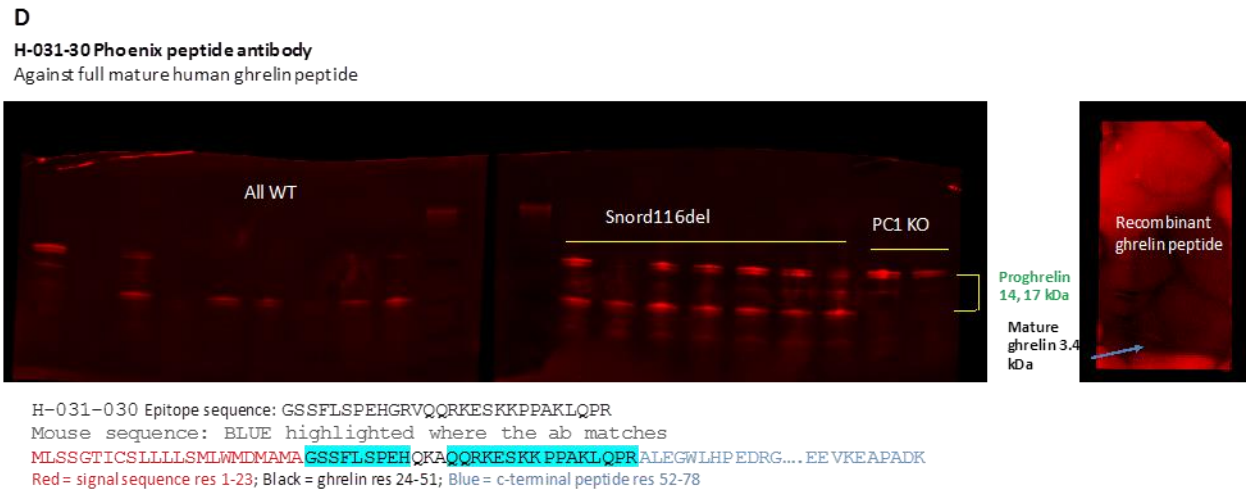

Supplemental Figure 15: Ghrelin western blot blotting identifies proghrelin reactivity of anti-ghrelin antibodies. A) Preproghrelin antibody is specific to preproghrelin and proghrelin peptides, 14 kDa and 17 kDa, respectively; no band is detected at 3.4 kDa, the size of mature ghrelin. B) The Santa Cruz C-18 anti-ghrelin antibody detects both mature ghrelin at 3.4 kDa and weakly reacts with proghrelin and preproghrelin at 14 and 17 kDa, respectively. C) The Phoenix Peptide H-031-31 anti-ghrelin (mouse) antibody detects proghrelin peptides and can detect an increase in proghrelin in Snord116$^{p-/m+}$ and PC1 null mice. H-031-31 is also used in the Phoenix Peptide RK-031-31 ghrelin rat, mouse RIA kit that has been previously used by other groups to detect increased circulating ghrelin in Snord116$^{p-/m+}$ mice compared to WT (*12*). D) The Phoenix Peptide H-031-30 anti-ghrelin (human) antibody also detects proghrelin peptides and can detect an increase in proghrelin in Snord116$^{p-/m+}$ and PC1 null mice compared to WT. This antibody is also used in the Pheonix Peptide RK-031-30 RIA kit that has been used in multiple studies of human plasma that detected 'hyperghrelinemia' in PWS as well as decreased circulating 'ghrelin' in common human obesity (*37-41*). It is possible that the hyperghrelinemia reported in PWS may be reflective of hyperproghrelinemia (W = wild type, PKO = PC1 null, D = Snord116 deletion; n=9 W; n=7 D; n=2 PKO; adult mice fasted overnight).

Supplemental Figure 16

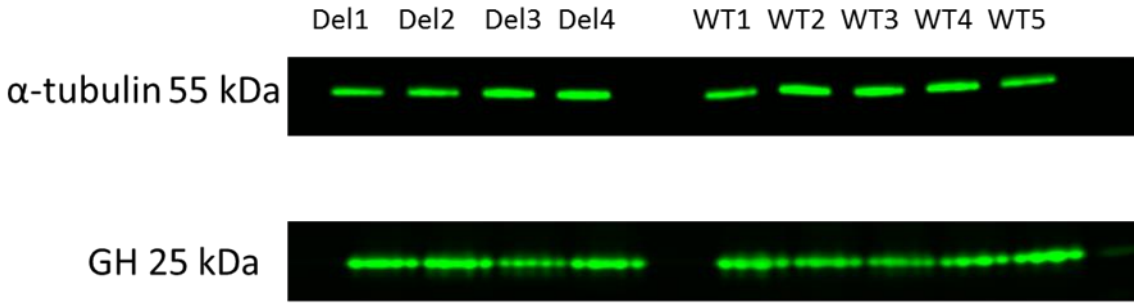

Supplemental Figure 16: There is no change in pituitary growth hormone levels in Snord116$^{p-/m+}$ mice compared to WT littermates at 1 month of age. Quantification is shown in Main Text figure 4 (n=5 WT; n=4 Del).

Supplemental Figure 17

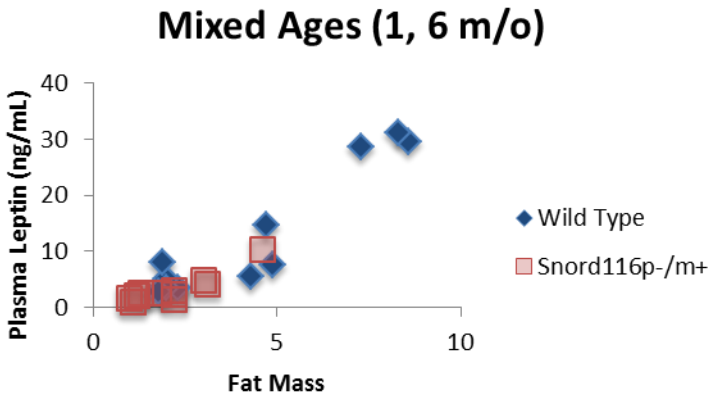

Supplemental Figure 17: Leptin is produced in proportion to fat mass in *Snord116*$^{p-/m+}$ mice. Leptin production is appropriate for fat mass levels in *Snord116*$^{p-/m+}$ mice as is seen when plasma leptin is plotted against fat mass (fat mass is measured in grams). Mice are either 1 month or 6 months of age; n=13 *Snord116*$^{p-/m+}$ male mice, n=13 WT male mice; plasma collected for leptin measurement under *ad lib* feeding conditions.

Supplemental References

1. M. A. Angulo, M. G. Butler, M. E. Cataletto, Prader-Willi syndrome: a review of clinical, genetic, and endocrine findings. *J Endocrinol Invest* **38**, 1249-1263 (2015).
2. T. Sahoo *et al.*, Prader-Willi phenotype caused by paternal deficiency for the HBII-85 C/D box small nucleolar RNA cluster. *Nature Genetics* **40**, 719-721 (2008).
3. A. J. de Smith *et al.*, A deletion of the HBII-85 class of small nucleolar RNAs (snoRNAs) is associated with hyperphagia, obesity and hypogonadism. *Human molecular genetics* **18**, 3257-3265 (2009).
4. A. L. Duker *et al.*, Paternally inherited microdeletion at 15q11.2 confirms a significant role for the SNORD116 C/D box snoRNA cluster in Prader-Willi syndrome. *European journal of human genetics : EJHG* **18**, 1196-1201 (2010).
5. E. Bieth *et al.*, Highly restricted deletion of the SNORD116 region is implicated in Prader-Willi Syndrome. *Eur J Hum Genet* **23**, 252-255 (2015).
6. M. G. Butler, S. L. Christian, T. Kubota, D. H. Ledbetter, A 5-Year-Old White Girl with Prader-Willi Syndrome and a Submicroscopic Deletion of Chromosome 15q11q13. *American Journal of Medical Genetics* **65**, 137-141 (1996).
7. P. Stijnen, B. Ramos-Molina, S. O'Rahily, J. W. M. Creemers, PCSK1 mutations and human endocrinopathies: from obesity to gastrointestinal disorders. *Endocrine Reviews* **17**, (2016).
8. X. Zhu *et al.*, Disruption of PC1/3 expression in mice causes dwarfism and multiple neuroendocrine peptide processing defects. *Proceedings of the National Academy of Sciences of the United States of America* **99**, 10293-10298 (2002).
9. X. Zhu, Y. Cao, K. Voogd, D. F. Steiner, On the processing of proghrelin to ghrelin. *The Journal of biological chemistry* **281**, 38867-38870 (2006).
10. D. J. Lloyd, S. Bohan, N. Gekakis, Obesity, hyperphagia and increased metabolic efficiency in Pc1 mutant mice. *Human molecular genetics* **15**, 1884-1893 (2006).
11. F. D. P. Deborah J. Good, Kathleen A. Mahon, Albert F. Parlow, Heiner Westphal, Ilan R. Kirsch, Hypogonadism and obesity in mice with a targeted deletion of the Nhlh2 gene. *Nature Genetics* **15**, 397-401 (1997).
12. F. Ding *et al.*, SnoRNA Snord116 (Pwcr1/MBII-85) deletion causes growth deficiency and hyperphagia in mice. *PloS one* **3**, e1709-e1709 (2008).
13. C. A. Coyle. *et al.*, Reduced voluntary activity precedes adult-onset obesity in Nhlh2 knockout mice. *Physiology & Behavior* **77**, 387-402 (2002).
14. A. M. Haqq, M. J. Muehlbauer, C. B. Newgard, S. Grambow, M. Freemark, The metabolic phenotype of Prader-Willi syndrome (PWS) in childhood: heightened insulin sensitivity relative to body mass index. *The Journal of clinical endocrinology and metabolism* **96**, E225-232 (2011).
15. X. Zhu. *et al.*, Severe block in processing of proinsulin to insulin accompanied by elevation of des-64,65 proinsulin intermediates in islets of mice lacking prohormone convertase 1/3. *Proceedings of the National Academy of Sciences* **99**, 10299–10304 (2002).
16. P. Stijnen *et al.*, Endoplasmic reticulum-associated degradation of the mouse PC1/3-N222D hypomorph and human PCSK1 mutations contributes to obesity. *International Journal of Obesity* **40**, 973-981 (2016).
17. J. C. Han, M. J. Muehlbauer, H. N. Cui, C. B. Newgard, A. M. Haqq, Lower Brain-Derived Neurotrophic Factor in Patients with Prader-Willi Syndrome Compared to Obese and Lean Control Subjects. *J Clin Endocrinol Metab* **95**, 3532-3536 (2010).
18. E. Vaiani *et al.*, Thyroid axis dysfunction in patients with Prader-Willi syndrome during the first 2 years of life. *Clinical Endocrinology* **73**, 546-550 (2010).
19. J. L. Miller *et al.*, Pituitary abnormalities in Prader-Willi syndrome and early onset morbid obesity. *American Journal of Medical Genetics* **146A**, 570-577 (2008).
20. M. G. Butler, M. Theodoro, J. D. Skouse, Thyroid Function Studies in Prader-Willi Syndrome. *American Journal of Medical Genetics Part A* **143A**, 488-492 (2007).
21. K. R. Vella, A. S. Burnside, K. M. Brennan, D. J. Good, Expression of the hypothalamic transcription factor Nhlh2 is dependent on energy availability. *Journal of Neuroendocrinology* **19**, 499-510 (2007).
22. R. F. de Lind van Wijngaarden *et al.*, High prevalence of central adrenal insufficiency in patients with Prader-Willi syndrome. *J Clin Endocrinol Metab* **93**, 1649-1654 (2008).

23. E. Jing, E. A. Nillni, V. C. Sanchez, R. C. Stuart, D. J. Good, Deletion of the Nhlh2 transcription factor decreases the levels of the anorexigenic peptides alpha melanocyte-stimulating hormone and thyrotropin-releasing hormone and implicates prohormone convertases I and II in obesity. *Endocrinology* **145**, 1503-1513 (2004).
24. W. T. Powell *et al.*, A Prader–Willi locus lncRNA cloud modulates diurnal genes and energy expenditure. *Human Molecular Genetics* **22**, 4318-4328 (2013).
25. U. D. Wankhade, K. R. Vella, D. L. Fox, D. J. Good, Deletion of Nhlh2 Results in a Defective Torpor Response and Reduced Beta Adrenergic Receptor Expression in Adipose Tissue. *PLoS One* **5**, e12323 (2010).
26. R. A. Harrington, D. A. Weinstein, J. L. Miller, Hypoglycemia in Prader-Willi syndrome. *Am J Med Genet A* **164A**, 1127-1129 (2014).
27. D. L. Fox, Dissertation, University of Massachusetts Amherst, Ann Arbor, MI (2007).
28. M. G. Butler *et al.*, Decreased bone mineral density in Prader-Willi syndrome: comparison with obese subjects. *American Journal of Medical Genetics Part A* **103**, 216-222 (2001).
29. T. Odent *et al.*, Scoliosis in Patients With Prader-Willi Syndrome. *Pediatrics* **122**, 1-7 (2008).
30. Y. Stelzer, I. Sagi, O. Yanuka, R. Eiges, N. Benvenisty, The noncoding RNA *IPW* regulates the imprinted *DLK-DIO3* locus in an induced pluripotent stem cell model of Prader-Willi syndrome. *Nature Genetics* **46**, 551-557 (2014).
31. L. Wang *et al.*, Differentiation of hypothalamic-like neurons from human pluripotent stem cells. *The Journal of Clinical Investigation* **125**, 796-808 (2015).
32. G. Sun *et al.*, Small C-terminal Domain Phosphatase 3 Dephosphorylates the Linker Sites of Receptor-regulated Smads (R-Smads) to Ensure Transforming Growth Factor β (TGFβ)-mediated Germ Layer Induction in Xenopus Embryos. *The Journal of Biological Chemistry* **290**, 17239-17249 (2015).
33. M. Ejarque *et al.*, Generation of a Conditional Allele of the Transcription Factor Atonal Homolog 8 (Atoh8). *PLoS One* **11**, e0146273 (2016).
34. K. Guo, Y.-H. Yu, J. Hou, Y. Zhang, Chronic leucine supplementation improves glycemic control in etiologically distinct mouse models of obesity and diabetes mellitus. *Nutrition & Metabolism* **7**, 1-10 (2010).
35. G. Stratigopoulos *et al.*, Hypomorphism for RPGRIP1L, a ciliary gene vicinal to the FTO locus, causes increased adiposity in mice. *Cell Metabolism* **19**, 767-779 (2014).
36. A. M. Abdellatif *et al.*, Role of large MAF transcription factors in the mouse endocrine pancreas. *Experimental Animals* **64**, 305-312 (2015).
37. T. M *et al.*, Circulating ghrelin levels are decreased in human obesity. *Diabetes* **50**, 707-709 (2001).
38. A. M. Haqq *et al.*, Circulating ghrelin levels are suppressed by meals and octreotide therapy in children with Prader-Willi syndrome. *J Clin Endocrinol Metab* **88**, 3573-3576 (2003).
39. A. P. Goldstone *et al.*, Elevated fasting plasma ghrelin in prader-willi syndrome adults is not solely explained by their reduced visceral adiposity and insulin resistance. *J Clin Endocrinol Metab* **89**, 1718-1726 (2004).
40. A. DelParigi *et al.*, High circulating ghrelin: a potential cause for hyperphagia and obesity in prader-willi syndrome. *J Clin Endocrinol Metab* **87**, 5461-5464 (2002).
41. E. Feigerlova *et al.*, Hyperghrelinemia precedes obesity in Prader-Willi syndrome. *The Journal of clinical endocrinology and metabolism* **93**, 2800-2805 (2008).